Supporting Information

Hurley et al. 10.1073/pnas.1203525109

SI Materials and Methods

RNA Isolation and Real-Time Reverse Transcription/PCR Assays. Total RNA was purified using the RNeasy Minikit (Qiagen). First-strand cDNA was synthesized using random hexamer primers (Applied Biosystems) and Ready-To-Go You-Prime First-Strand Beads (GE Healthcare), according to the manufacturers' instructions. Quantitative PCR was performed using iQ SYBR Green Supermix (BioRad), with primers specific to human SPARCL1 set one F/R: (5′GTTCCTTCACAGATTCTAACCA3′) (5′TTTACTGCTCCTGTTCAACTG3′); set two F/R: (5′ATCATTCCAAACCAACTGCT3′) (5′GACTGTTCATGGCTTTCCTC3′). Bio-Rad MyiQ software was used to calculate threshold cycle values for secreted protein, acidic and rich in cysteine-like 1 (SPARCL1) and the reference gene hypoxanthine phosphoribosyltransferase (HPRT). Quantitative PCR was performed using TaqMan Universal PCR Master Mix (Applied Biosystems) with TaqMan primers specific to mouse Sparcl1 (Applied Biosystems). Applied Biosystems software was used to calculate threshold cycle values for Sparcl1 and the reference gene HPRT.

In Vitro Organ Culture. The protocol was approved by The Johns Hopkins University Animal Care and Use Committee. The urogenital sinus (UGS) was harvested from embryonic day (E) 15.5 males and then incubated in UGS media: DMEM-F12 (Invitrogen), Nonessential amino acids (Cellgro), ITS media (Sigma), Pen/Strep (Invitrogen), 1 g/L D-glucose (Sigma), and L-Glutamine (Invitrogen) with recombinant murine Sparcl1 (mSparcl1) (10 μg/mL) (R&D Systems; 4547-SL) or vehicle for 2 h at 4 °C. The UGS was placed (ventral side up) on a 0.4-μm Millicell filter (Millipore) in a six-well plate with UGS media supplemented with 10^{-8} M dihydrotestosterone (DHT) and vehicle or recombinant mSparcl1 (10 μg/mL). Media was changed every 24 h.

Immunohistochemistry, Immunofluorescence, and Immunoblotting. For immunohistochemistry (IHC) and immunofluorescence (IP), tissues were fixed in 10% (vol/vol) neutral buffered formalin (NBF), embedded in paraffin, sectioned, deparaffinized, steamed in Target Retrieval Solution Ready to Use (Dako) for 40 min, blocked with Protein Block Serum-Free (Dako), incubated with antibodies directed against CK8 (Covance; MMS-162P, 1:500–1,000), CK14 (Covance; PRB155P, 1:300), pancytokeratin (Sigma; C2562, 1:400), p63 (Millipore; MAB4135, 1:100), SPARCL1 for mouse and human (Abcam; Ab-107533, 1:500), and Ki67 (Abcam; Ab-15580, 1:100) in Antibody Diluent (Invitrogen). Antibodies to SPARCL1 were comprehensively tested in accordance with The Johns Hopkins Brady Urological Research Institute Prostate Specimen Repository protocols. IHC was detected with 3,3′-Diaminobenzidine kit (Vector Laboratories). For IF, primary antibodies were followed by Alexa Fluor Dye secondary antibodies (Invitrogen) and mounted with Vectashield hard-set mounting medium with DAPI counterstain (Vector Laboratories). Images were captured at room temperature on a Nikon E800 fluorescence microscope with 40× Plan Apo objective and a Nickon DS-QiMc camera with Nikon Elements imaging software (vAR 3.0).

For immunoblotting (IB), lysates were fractionated on NuPAGE gels (Invitrogen). Proteins were transferred to polyvinylidene difluoride membranes, blocked, and then incubated with antibodies directed against SPARCL1 (Abcam; Ab-107533, 1:1,000), GAPDH (Santa Cruz; Sc-32233, 1:5,000), RhoA (Santa Cruz; Sc-418, 1:1,000), and RhoC (Cell Signaling Technology; 3430, 1:1,000) according to the manufacturers' recommendations. Blots were developed using enhanced chemiluminescence (Thermo Fisher Scientific) or Odyssey IRDye (LI-COR Biosciences).

Prostate Regeneration. The protocol was approved by The Johns Hopkins University Animal Care and Use Committee. C57Bl6/J mice obtained from The Jackson Laboratory were castrated, rested for 14 d, and treated with daily subcutaneous vehicle [80% (vol/vol) glycerol trioleate in ethanol] alone or with DHT (50 mg/kg). Prostates were collected from killed animals and processed for histology or for RNA purification (Qiagen).

Three-Dimensional Prostate Invasion Assay. The protocol was approved by The Johns Hopkins University Animal Care and Use Committee. Prostates were harvested from adult killed C56BL6 mice obtained from The Jackson Laboratory, minced with a razor blade, and dissociated with 0.5% collagenase type II (Sigma) in DMEM (Invitrogen) with 10% (vol/vol) FCS (Gemini Bio-Products) for 60 min at 37 °C with shaking. Cell clumps were pipetted every 15 min during digestion. Cells were centrifuged and resuspended in 0.25% trypsin for 10 min at 37 °C, washed with PBS, resuspended in DMEM with 10% (vol/vol) FCS, plated on a 6-cm plate, and incubated for 2 h at 37 °C with 5% CO_2. Nonadherent cells were passed through a 40-μm nylon mesh, washed with PBS, resuspended in epithelial basal medium (PrEBM) (Lonza), and counted. Next, 20,000 cells in PrEBM plus recombinant mSparcl1 (10 μg/mL) (R&D Systems) or vehicle were mixed with an equal amount of Matrigel (BD Biosciences), plated around the rim of a well of a 12-well plate, allowed to solidify for 30 min at 37 °C with 5% CO_2, and then treated with recombinant mSparcl1 (10 μg/mL) or vehicle in PrEBM. Media was changed every 24 h. Prostaspheres were isolated from the Matrigel with Dispase (BD Biosciences) for 30 min at 37 °C, washed with PBS, fixed in 10% (vol/vol) NBF, washed with PBS, embedded in 2% (wt/vol) agarose, and processed for histology. Five hundred prostate epithelial cells (PrEC) cells were used in the above protocol for PrEC prostasphere formation.

Cell Growth, Cell Cycle, and Apoptosis Assays. Cell growth in PC3, DU145, and CWR22RV1 was assayed by incubating cells in Thiazolyl Blue Tetrazolium Bromide (MTT) for 5 min at room temperature with shaking and then at 37 °C for 1 h. Cells were then incubated in DMSO for 5 min at room temperature with shaking and optical density was read at 570 and 690 nm.

To assay the cell cycle, PC3 were treated with recombinant human SPARCL1 (hSPARCL1) (10 μg/mL) (R&D Systems; 2728-SL) and nocodazole (to induce G2/M arrest) for 0, 6, and 18 h. Cells were collected by incubation in trypsin/ethylenediaminetetraacetic acid, pelleted by centrifugation, and fixed in PBS containing 3.7% (vol/vol) formaldehyde, 0.5% Nonidet P-40, and 10 μg/mL Hoechst 33258. A total of 10,000 cells were analyzed per sample on a flow cytometer (LSRII; Applied Biosystems).

Proliferation in PC3 cells was assayed using the Click-iT EdU Cell Proliferation Assay according to the manufacturer's recommendation (Invitrogen). A total of 10,000 cells were analyzed per sample on a flow cytometer (LSRII; Applied Biosystems).

Cell death in PC3 cells was analyzed according to the manufacturer's recommendation of the Vybrant Apoptosis Assay Kit with FITC Annexin (Invitrogen). A total of 10,000 cells were analyzed per sample on a flow cytometer (FACSCaliber; BD Biosciences).

Cell Culture. We used multiple human prostate cancer cell lines lacking SPARCL1 expression (Fig. 5*A* and Fig. S6*H*). Human

prostate cancer cell lines PC3, CWR22RV1, and DU145 (all gifts from John Isaacs, The Johns Hopkins University, Baltimore, MD), and LNCaP (American Type Culture Collection) cells were cultured in growth media (RPMI-1640 supplemented with 10% (vol/vol) FBS). Human primary prostate epithelial cells PrEC (Lonza) were cultured in growth media (PrEBM; Lonza).

Adhesion, Migration, and Invasion Assays. Cell adhesion was assayed in PC3, CWR22RV1, DU145, LNCaP, and PrEC cells. An equal number of cells were seeded on type I collagen/vehicle- or type I collagen/SPARCL1-coated plates. Cell adhesion was monitored and photographed using a light microscope. Cell migration was assayed using the Cell Migration Colorimetric Assay Kit (Millipore) according to the manufacturer's instructions. Cell invasion was assayed using the QCM ECMatrix Colorimetric Cell Invasion Assay (Millipore) and the QCM Collagen Colormetric Cell Invasion Assay (Millipore), according to the manufacturer's instructions. PC3 cells were seeded on type I collagen/vehicle- or type I collagen/SPARCL1-dually coated plates and photographed every 5 min for 22 h using Incucyte (Essen Bioscience) and analyzed for proliferation, adhesion, and migration with Incucyte software. PC3 cells were transfected with Ras homolog gene family, member C (RHOC) (Missouri S&T Resource Center) or RHOC G14V (Missouri S&T Resource Center) using FuGENE (Roche) according to the manufacturer's instructions, and then assayed for cell migration using the Cell Migration Colorimetric Assay Kit (Millipore).

Activated Rho Assay. Ten-centimeter type I collagen-coated plates (BD Biosciences) were coated overnight with 10 μg/mL recombinant hSPARCL1 (R&D Systems) or BSA at 4 °C. PC3 cells were then plated on these plates for 6 h or until equally adherent. Cells were washed twice with ice cold TBS and lysed in 1 mL Rho Buffer (25 mM Hepes, 150 mM NaCl, 1% Igpal, 10 mM MgCl2, 1 mM EDTA, 2% (vol/vol) glycerol, PMSF, Sigma protease inhibitor mixture) for 15 min at 4 °C with agitation, passed through a fine-gauge needle, cleared by centrifugation, and then incubated with Rhotekin-RBD Protein GST Beads (Cytoskeleton) overnight at 4 °C with rotation. Both pre-IP and post-IP lysates were collected for analysis. IP lysates were washed three times with ice-cold Rho Buffer and then incubated at 70 °C for 10 min in 1× NuPage Lysis buffer (Invitrogen) containing PMSF and Sigma protease inhibitor mixture. PC3 cells were transiently transfected with pcDNA3.1- or hSPARCL1/pcDNA3.1- (Thermo Scientific) using FuGENE (Roche) according to the manufacturer's instructions. Following transfection, cells were incubated with $IgG1_k$ (BD Pharmingen) or a blocking antibody to α2β1 (Millipore) for 6 h on type 1 collagen plates.

TRAMP Mice and Hi-Myc Mice. The protocol was approved by the Johns Hopkins University Animal Care and Use Committee. Tissue was obtained from adult killed C57BL/6/FVB F1 transgenic adenocarcinoma of the mouse prostate (TRAMP) mice (shown), C57BL/6 TRAMP mice and FVB Hi-Myc mice, fixed with 10% (vol/vol) neutral buffered formalin, paraffin embedded, and sectioned for IHC.

Johns Hopkins University Prostate Cancer Gleason Grade Tissue Microarrays. Tissue microarrays (TMAs) were constructed from archival tissue from radical prostatectomies performed at The Johns Hopkins University (JHU) between 2000 and 2001. Cases for the TMA were reviewed and selected by a genitourinary pathologist. The largest tumor of the highest grade was selected. In each case, the index tumors of Gleason sum 5, 6, 8, and 9 were spotted in triplicate. Benign adjacent glands were also obtained and spotted in triplicate. Four-micrometer-cut sections were stained for SPARCL1 by IHC, as described above. A total of 58 cases were scored by a urologic pathologist for SPARCL1 expression: benign adjacent (n = 20), Gleason sum 5 (n = 4), Gleason sum 6 (n = 16), Gleason sum 8 (n = 10), and Gleason sum 9 (n = 8). Using an established scoring scheme, SPARCL1-staining intensity was evaluated and assigned an incremental score of 0 (low or absent), 1 (medium), or 2 (strong) (1). The extent of staining was assigned a score for 0–33% (score 0), 34–66% (score 1), or 67–100% (score 2). For each sample, a SPARCL1 score was calculated by adding the intensity score and the extent score (H-score). H-scores were compared using the one-way ANOVA test with the Bonferroni's post hoc pairwise comparison test. Statistical analyses were performed using GraphPad Software. Statistical tests were two sided and P values less than 0.05 were considered statistically significant.

JHU Progression TMA: Construction, IHC Staining, and Scoring. The design of the nested case-control study of prostate cancer recurrence has been described previously (2). Briefly, included were men who underwent radical prostatectomy (RP) for clinically localized prostate cancer at The Johns Hopkins Medical Institutions between 1993 and 2004 and who had not had hormonal or radiation therapy before radical prostatectomy or adjuvant therapy before recurrence. Cases were men who experienced biochemical recurrence as measured by a reelevation of serum prostate-specific antigen (PSA) ≥0.2 ng/mL, metastasis, or prostate cancer death after surgery (Fig. S7*A*). For each case, a control was selected who had not experienced recurrence by the date of the cases' recurrence and who was matched on age, race, pathological stage, and Gleason's sum. Tumors from matched pairs were spotted (0.6 mm) in quadruplicate on the same TMA, which is a strategy that has been shown to provide optimal predictive value for the prostate (2). In cases with multifocal tumors, only the index tumor (the dominant tumor with the highest Gleason's sum and usually the largest) was included. Based on a priori sample size calculations, four TMAs were used. One 4-μm section cut from each TMA was stained for SPARCL1, as described above. The extent and intensity of SPARCL1 staining was determined by urologic pathologists using digitized TMAJ software. A single score, called the H-score, which integrated both the extent and intensity of SPARCL1 staining, was digitally computed by TMAJ software for each core. After exclusion of technically inadequate TMA cores and men with less than three TMA cores, the final analysis included 68 cases and 68 matched controls. Conditional logistic regression was used to estimate the odds ratio of recurrence taking into account the matching factors and adjusting for year of surgery, presurgical PSA level, positive surgical margins, and residual difference in pathologic stage and grade. We categorized each TMA core for each man as being below or at/or above the median H-score (calculated among all of the cores for all of the controls included on the four TMAs). Analyses were performed using SAS version 9.1 (SAS Institute). Statistical tests were two-sided and P values less than 0.05 were considered to be statistically significant.

Mayo Clinic Progression Analyses: Study Design, Tissue Preparation, RNA Extraction, Microarray Hybridization and Microarray Expression Analysis, and Statistical Analysis. ***Study design.*** Patients were selected from a cohort of high-risk RP patients from the Mayo Clinic with a median follow-up of 8.1 y. The cohort was defined as 1,010 high-risk men who underwent RP between 2000 and 2006, of which 73 patients developed metastatic disease as evidenced by positive bone or CT scan. High-risk cohort was defined as preoperative PSA >20 ng/mL, pathological Gleason score 8–10, seminal vesicle invasion, or GPSM (Gleason, prostate specific antigen, seminal vesicle and margin status) score ≥10 (2). The subcohort incorporated all 73 metastatic patients and a 20% random sampling of the entire cohort; of these, tissue specimens were available for 235 patients (n = 235). This subcohort was previously used to validate a genomic classifier for predicting metastatic disease at RP (5).

Tissue preparation. Formalin-fixed paraffin embedded (FFPE) samples of human prostate adenocarcinoma prostatectomies were collected from patients at the Mayo Clinic according to an institutional review board-approved protocol. Pathological review of H&E tissue sections was used to guide macrodissection of tumor from surrounding stromal tissue from three to four 10-μm sections. The index lesion was considered the dominant lesion by size.

RNA extraction and microarray hybridization. For the validation cohort, total RNA was extracted and purified using a modified protocol for the commercially available RNeasy FFPE nucleic acid extraction kit (Qiagen). RNA concentrations were calculated using a Nanodrop ND-1000 spectrophotometer (Nanodrop Technologies). Purified total RNA was subjected to whole-transcriptome amplification using the WT-Ovation FFPE system, according to the manufacturer's recommendation with minor modifications (NuGen). For the validation only the Ovation FFPE WTA System was used. Amplified products were fragmented and labeled using the Encore Biotin Module (NuGen) and hybridized to Affymetrix Human Exon 1.0 ST GeneChips following the manufacturer's recommendations (Affymetrix).

Microarray expression analysis. The normalization and summarization of the microarray samples was done with the frozen robust multiarray average algorithm using custom frozen vectors. These custom vectors were created using the vector creation methods, as described previously (6). Quantile normalization and robust weighted-average methods were used for normalization and summarization, respectively, as implemented in frozen robust multiarray average.

Statistical analysis. Given the exon/intron structure of *SPARCL1*, all probe selection regions (or PSRs) that fall within the genomic span of *SPARCL1* were inspected for overlapping this gene. One PSR, 277167, was used for further analysis as a representative PSR for this gene. The partition around the medoid unsupervised clustering method was used on the expression values of all clinical samples to define two groups of high and low expression of *SPARCL1*. Statistical analysis on the association of *SPARCL1* with clinical outcomes was done using three endpoints: (*i*) Biochemical recurrence (BCR), defined as two consecutive increases of ≥0.2 ng/mL PSA after RP; (*ii*) Metastasis (MET), as defined by a positive bone scan or CR/MRI evidence of metastatic disease; and (*iii*) Prostate cancer-specific mortality (PCSM). For the MET-free survival end point, all patients with metastasis were included in the survival analysis, whereas the controls in the subcohort were weighted in a fivefold manner to be representative of patients from the original cohort. For the PCSM end point, patients from the cases who did not die by prostate cancer were omitted, and weighting was applied in a similar manner. For BCR, because the case-cohort was designed based on a MET-free survival endpoint, resampling of BCR patients and subcohort was done to have a representative of the selected BCR patients from the original cohort.

Other Statistical Analysis. Statistical analyses were performed using GraphPad Software. Statistical tests were two sided and *P* values less than 0.05 were considered statistically significant.

1. Schultz L, et al. (2010) Expression status and prognostic significance of mammalian target of rapamycin pathway members in urothelial carcinoma of urinary bladder after cystectomy. *Cancer* 116:5517–5526.
2. Toubaji A, et al. (2011) Increased gene copy number of ERG on chromosome 21 but not TMPRSS2-ERG fusion predicts outcome in prostatic adenocarcinomas. *Mod Pathol* 24: 1511–1520.
3. Rubin MA, Dunn R, Strawderman M, Pienta KJ (2002) Tissue microarray sampling strategy for prostate cancer biomarker analysis. *Am J Surg Pathol* 26:312–319.
4. Blute ML, Bergstralh EJ, Iocca A, Scherer B, Zincke H (2001) Use of Gleason score, prostate specific antigen, seminal vesicle and margin status to predict biochemical failure after radical prostatectomy. *J Urol* 165:119–125.
5. Buerki C, et al. (2012) Validation of a genomic-clinical classifier for predicting clinical progression in high-risk prostate cancer. *Journal of Clinical Oncology* 30(May 20 Suppl): 4565.
6. Vergara IA, et al. (2012) Genomic "Dark Matter" in prostate cancer: Exploring the clinical utility of ncRNA as biomarkers. *Front Gen* 3:23.

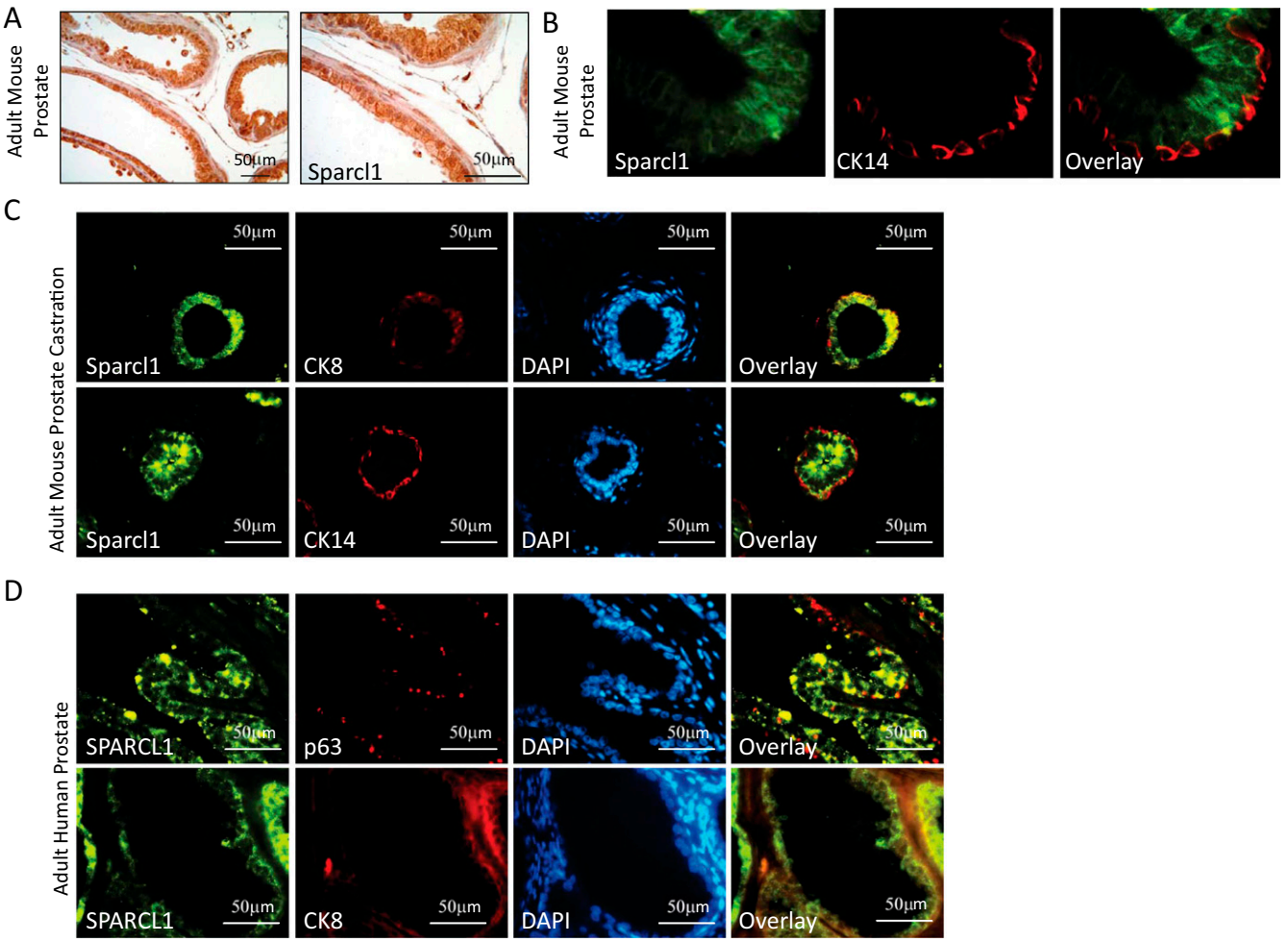

Fig. S1. Sparcl1 protein expression is increased in prostate epithelial cells following castration. (*A*) Sparcl1 expression in the adult mouse prostate as determined by IHC. (*B*) Sparcl1 expression occurs in a subpopulation of basal cells as determined by immunofluorescence (IF) colocalization with CK14 in adult mouse prostate. Magnification, 400×. (*C*) Increased Sparcl1 protein expression following castration (3 wk) occurs predominantly in luminal prostate epithelial cells as determined by IF colocalization with CK8 and CK14. (*D*) SPARCL1 protein expression in adult human benign prostate as determined by IF colocalization with p63 and CK8.

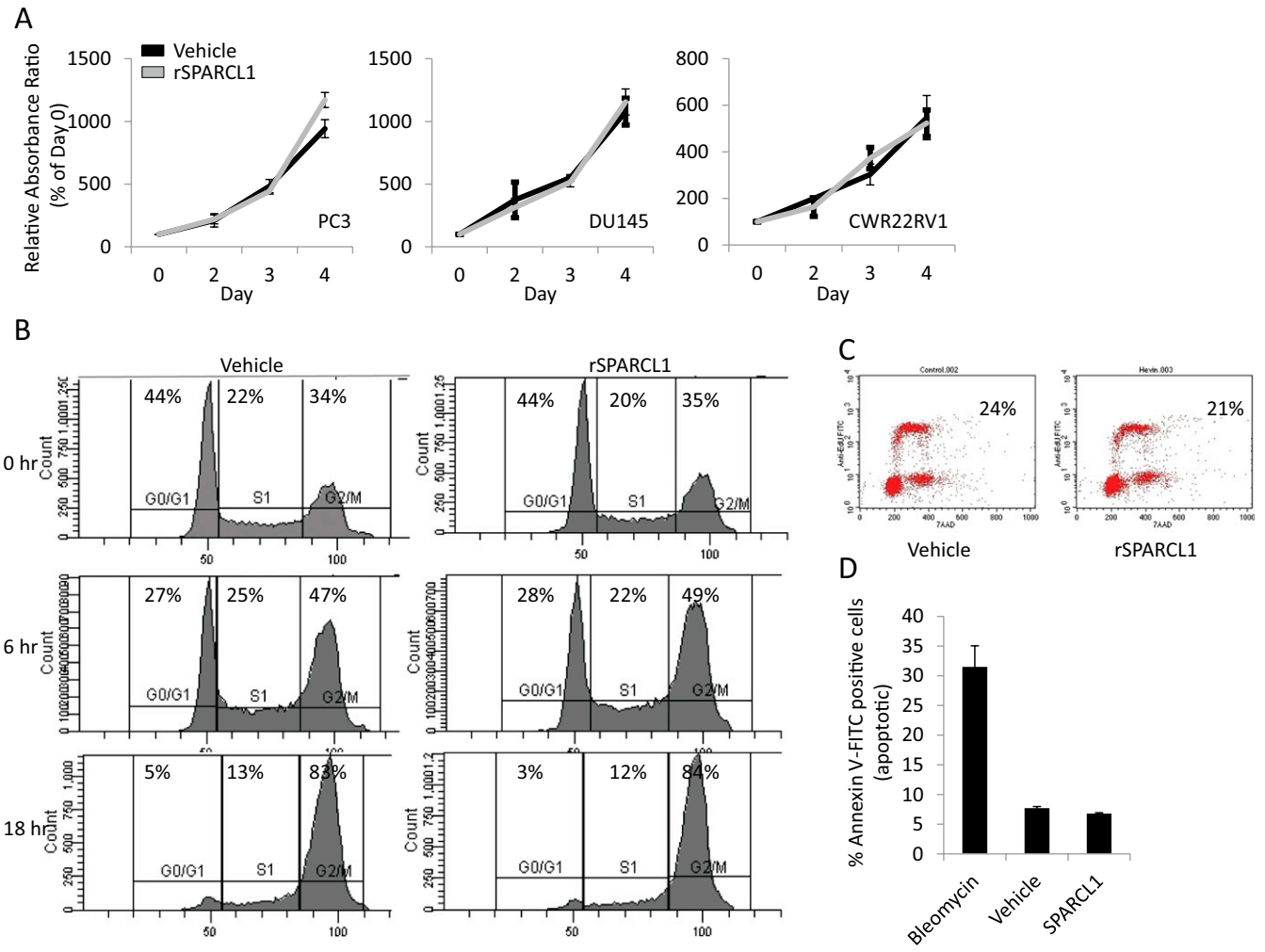

Fig. S2. SPARCL1 does not affect cellular proliferation or death in human prostate cancer cell lines. (*A*) SPARCL1 does not affect cell growth in human prostate cancer cell lines. PC3, DU145, and CWR22RV1 cells were treated with vehicle or recombinant hSPARCL1 (10 μg/mL) for 0, 2, 3, and 4 d. Cell growth was analyzed by MTT assay (mean ± SD; $n = 3$). (*B*) SPARCL1 does not affect cell cycle progression in prostate cancer cells. Asynchronous PC3 cells were treated with vehicle or recombinant hSPARCL1 (10 μg/ml) for 24 h. All cultures were then treated with the microtubule inhibitor nocodazole to block cells in mitosis and thereby preventing nascent cells from re-entering the 2N population. Cell cycle distribution was measured by flow cytometry. (*C*) SPARCL1 does not affect DNA synthesis in prostate cancer cells. PC3 cells were treated with vehicle or recombinant hSPARCL1 (10 μg/ml) for 24 h, incubated with 5-ethynyl-2′-deoxyruidine (EdU), and then examined by flow cytometry for EdU incorporation as a measure of DNA synthesis and S-phase progression. (*D*) SPARCL1 does not cause apoptosis in prostate cancer cells. PC3 cells were treated with vehicle, recombinant hSPARCL1 (10 μg/mL), or Bleomycin (200 μg/mL) for 48 h. Cell death was examined by flow cytometry following annexin staining (mean ± SD; $n = 3$).

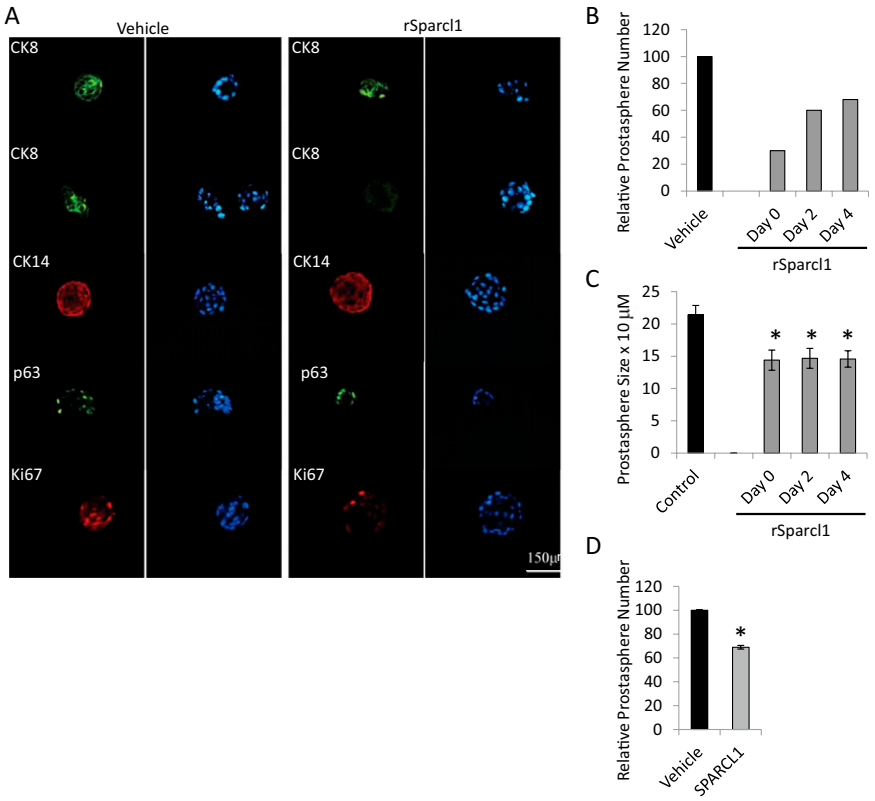

Fig. S3. Sparcl1 inhibits prostasphere formation following initiation. (*A*) Sparcl1 does not inhibit prostasphere proliferation or differentiation as analyzed by IF for Ki67 (proliferation) and CK8, CK14, and p63 (differentiation) in vehicle- and recombinant mSparcl1- (10 μg/mL) treated prostaspheres. Despite overall differences in size between vehicle- and Sparcl1-treated prostaspheres, sections of approximate equal diameter were chosen for comparable analysis of differentiation and proliferation markers. (*B* and *C*) Adult mouse prostate epithelial cells established in Matrigel for 0, 2, or 4 d before treatment with recombinant mSparcl1 (10 μg/mL) or vehicle (mean ± SD; $*P \leq 0.003$). (*D*) SPARCL1 restricts benign prostate epithelial prostasphere formation. Adult human primary benign PrEC from deceased organ donors, cultured in Matrigel, and treated with recombinant hSPARCL1 (10μg/mL) or vehicle for 14 d to form prostaspheres (mean ± SEM; $n = 4$; $*P \leq 0.001$). Statistical analysis performed by Student *t* test.

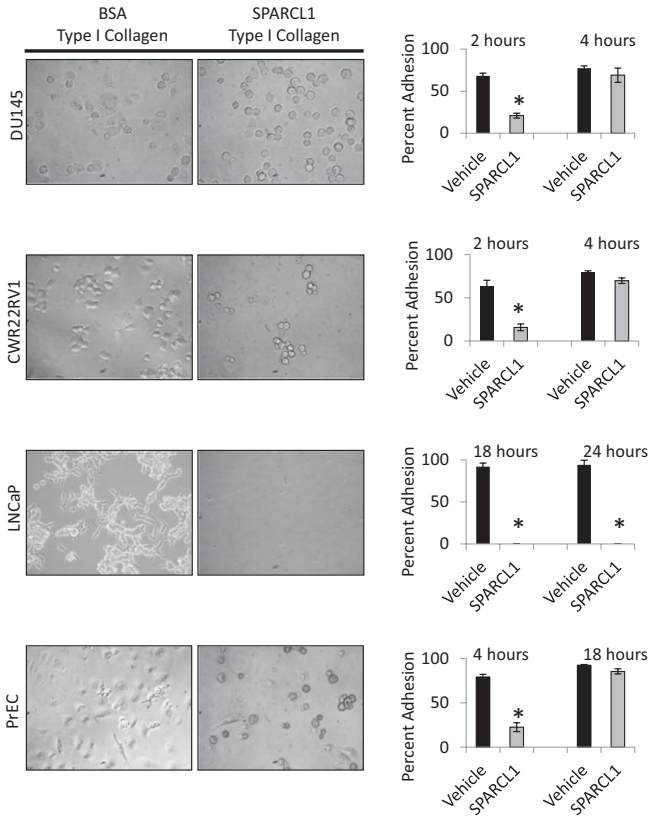

Fig. S4. SPARCL1 delays/abrogates prostate cancer cell adhesion to type I collagen. DU145, CWR22RV1, LNCaP, and PrEC cells were allowed to attach to a type I collagen/BSA (10 μg/mL) or a type I collagen/recombinant hSPARCL1 (10 μg/mL) matrix. Following incubation, plates were photographed and monitored for cellular adhesion. Abrogation of adhesion in LNCaP cells may be related to their relatively nonadherent nature compared with the other cell lines and cells. Statistical analysis performed by Student *t* test (mean ± SEM; $n \geq 3$; $^*P < 0.004$). (Magnification, 200×.)

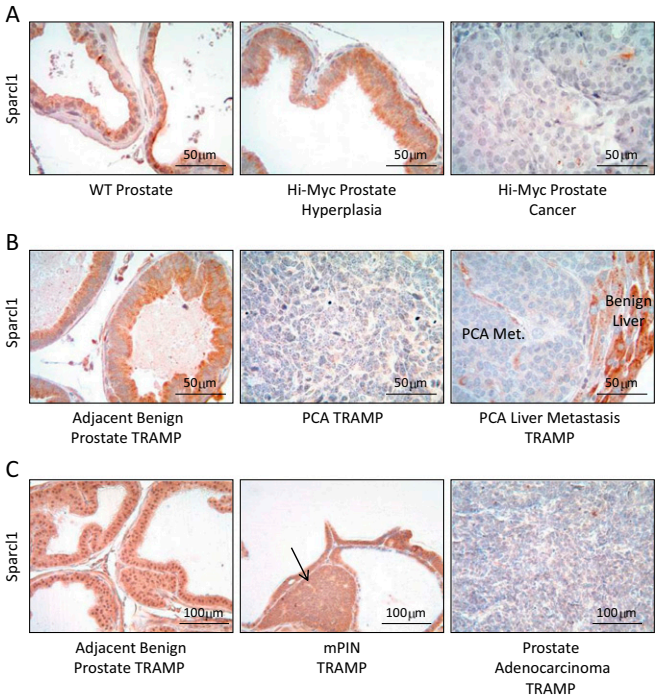

Fig. S5. Sparcl1 expression is decreased in animal models of prostate adenocarcinoma. (*A*) Sparcl1 expression is decreased in locally invasive primary prostate adenocarcinoma as examined by IHC in benign prostate adjacent to cancer, prostate hyperplasia, and primary prostate adenocarcinoma in Hi-Myc mice ($n = 4$). (*B*) Decreased Sparcl1 expression in primary prostate adenocarcinoma and metastatic lesions as determined by IHC in benign prostate adjacent to cancer, primary prostate adenocarcinoma, and metastatic lesions to the liver from TRAMP mice ($n = 5$). (*C*) Sparcl1 expression is decreased in primary prostate adenocarcinoma compared with benign adjacent glands and murine prostatic intraepithelial neoplasia (mPIN), as examined by IHC in benign prostate adjacent to cancer, mPIN, and primary prostate adenocarcinoma from TRAMP mice ($n = 5$).

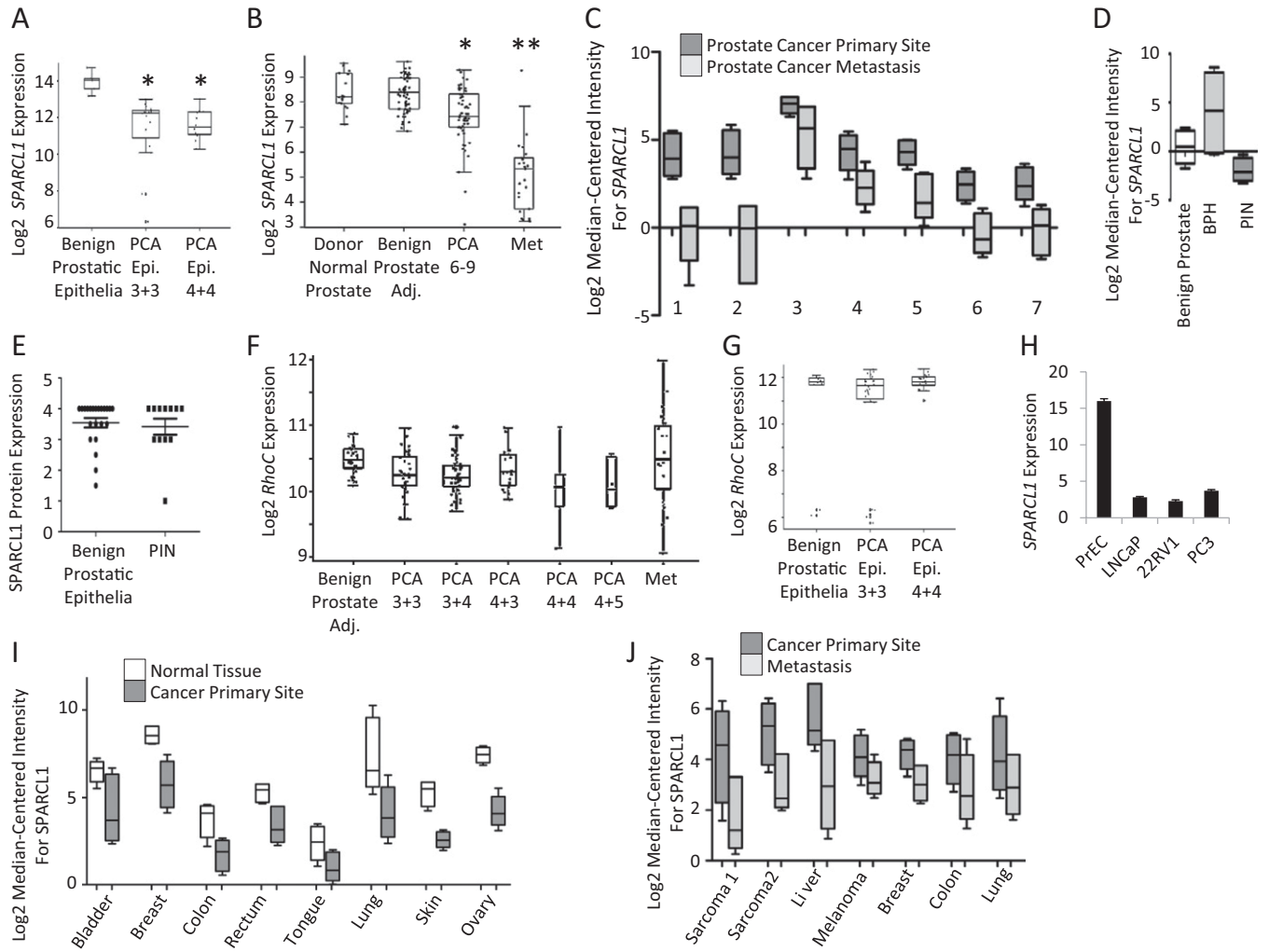

Fig. S6. *SPARCL1* gene expression inversely correlates with prostate cancer aggressiveness. (*A*) *SPARCL1* gene expression inversely correlates with prostate cancer Gleason grade. Analysis performed on data sets from Ross et al. (1) for *SPARCL1* gene expression. *Benign prostatic epithelial vs. prostate cancer (PCA) $P \leq 0.005$. (*B*) *SPARCL1* gene expression is inversely proportional to prostate cancer aggressiveness. One-way Anova analysis was performed on datasets from Chandran et al. (2) for SPARCL1 gene expression. *Donor normal vs. prostate carcinoma and **prostate carcinoma vs. metastatic prostate cancer $P \leq 0.00005$. (*C*) Data obtained from Oncomine (Compendia Bioscience) was used for analysis and visualization. In "1" Ramaswamy et al. (3), primary prostate tumor ($n = 10$) vs. metastasis ($n = 4$) $P = 0.008$. In "2" Ramaswamy et al. (4), primary prostate tumor ($n = 10$) vs. metastasis ($n = 3$) $P = 0.028$. In "3" Varambally et al. (5), primary prostate tumor ($n = 7$) vs. metastasis ($n = 6$) $P = 0.026$. In "4" Lapointe et al. (6), primary prostate cancer ($n = 62$) vs. metastasis ($n = 8$) $P = 5.79E\text{-}5$. In "5" LaTulippe et al. (7), primary prostate cancer ($n = 23$) vs. metastasis ($n = 9$) $P = 2.75E\text{-}5$. In "6" Holzbeierlein et al. (8), primary prostate cancer ($n = 40$) vs. metastasis ($n = 9$) $P = 4.41E\text{-}6$. In "7" Yu et al. (9), primary prostate cancer ($n = 64$) vs. metastasis ($n = 24$) $P = 1.71E\text{-}10$. (*D*) Data obtained from Oncomine (Compendia Bioscience) was used for analysis and visualization. In Tomlins et al. (10), *SPARCL1* gene expression is not altered significantly in benign prostatic hyperplasia (BPH) ($P = 0.771$) or PIN ($P = 0.054$) compared with benign epithelia adjacent to prostate cancer. (*E*) SPARCL1 expression as measured by IHC is not decreased significantly in hPIN ($n = 12$) compared with benign epithelia adjacent to prostate cancer ($n = 22$) $P = 0.652$. (*F* and *G*) *RHOC* gene expression does not correlate with prostate cancer Gleason grade. In silico analysis was performed on data sets from Taylor et al. (11) and Ross et al. (1) for *RHOC* gene expression. In Taylor et al. (11) (*F*), *RHOC* in benign prostate adjacent to cancer vs. PCA G3+3 $P = 0.032$, benign prostate adjacent to cancer vs. G3+4 $P = 0.013$, benign prostate adjacent to cancer vs. PCA G4+3 $P = 0.208$, benign prostate adjacent to cancer vs. PCA G4+4 $P = 0.018$, benign prostate adjacent to cancer vs. PCA G4+5 $P = 0.034$, and benign prostate adjacent to cancer vs. MET $P = 0.657$. In Ross et al. (1) (*G*), *RHOC* in benign prostatic epithelial vs. PCA epithelia G3+3 = 6 $P = 0.905$ and benign prostatic epithelial vs. PCA epithelia G4+4 = 8 $P = 0.106$. (*H*) *SPARCL1* gene expression is reduced in human prostate cancer cell lines compared with primary benign human PrEC. Expression of *SPARCL1* mRNA was determined by quantitative PCR in human prostate cell lines (LNCaP, 22RV1, and PC3) and in human primary PrEC from deceased organ donors. (*I*) *SPARCL1* gene expression inversely correlates with cancer aggressiveness in multiple solid malignancies. Data obtained from Oncomine (Compendia Bioscience) was used for analysis and visualization. In Sanchez-Carbayo et al. (12), normal bladder ($n = 48$) vs. infiltrating urothelial carcinoma ($n = 81$) $P = 5.09E\text{-}29$. In Richardson et al. (13), normal breast ($n = 7$) vs. ductal breast carcinoma ($n = 40$) $P = 4.07E\text{-}14$. In Notterman et al. (14), normal colon ($n = 18$) vs. colon adenocarcinoma ($n = 18$) $P = 3.44E\text{-}8$. In Sabates Bellver et al. (15), normal rectum ($n = 32$) vs. rectal adenoma ($n = 7$) $P = 4.70E\text{-}5$. In Estilo et al. (16), normal tongue ($n = 26$) vs. tongue squamous cell carcinoma ($n = 32$) $P = 1.50E\text{-}6$. In Bhattacharjee et al. (17), normal lung ($n = 17$) vs. lung adenocarcinoma ($n = 139$) $P = 5.33E\text{-}7$. In Talantov et al. (18), normal skin ($n = 7$) vs. cutaneous melanoma ($n = 45$) $P = 4.40E\text{-}6$. From Cancer Genome Atlas normal ovary vs. ovarian serous cystadenocarcinoma $P = 1.69E\text{-}10$. (*J*) *SPARCL1* gene expression is down-regulated in metastases compared with the primary tumor in multiple solid malignancies. Data obtained from Oncomine (Compendia Bioscience) was used for analysis and visualization. In Segal et al. (19), sarcoma 1 ($n = 29$) vs. metastasis ($n = 4$) $P = 0.009$. In Segal et al. (20), sarcoma 2 ($n = 46$) vs. metastasis ($n = 4$) $P = 0.007$. In Liao et al. (21), liver carcinoma ($n = 4$) vs. metastasis ($n = 6$) $P = 0.007$. In Xu et al. (22), melanoma ($n = 31$) vs. metastasis ($n = 52$) $P = 8.83E\text{-}5$. In Radvanyi et al. (23), breast carcinoma ($n = 47$) vs. metastasis ($n = 7$) $P = 2.4E\text{-}4$. In Ki et al. (24), colorectal cancer ($n = 52$) vs. metastasis ($n = 28$) $P = 3.28E\text{-}4$. In Bhattachargee et al. (17), lung cancer ($n = 123$) vs. metastasis ($n = 7$) $P = 0.004$.

1. Ross AE, et al. (2011) Gene expression pathways of high grade localized prostate cancer. *Prostate* 71:1568–1577.
2. Chandran UR, et al. (2005) Differences in gene expression in prostate cancer, normal appearing prostate tissue adjacent to cancer and prostate tissue from cancer free organ donors. *BMC Cancer* 5:45.
3. Ramaswamy S, et al. (2001) Multiclass cancer diagnosis using tumor gene expression signatures. *Proc Natl Acad Sci USA* 98:15149–15154.
4. Ramaswamy S, Ross KN, Lander ES, Golub TR (2003) A molecular signature of metastasis in primary solid tumors. *Nat Genet* 33:49–54.
5. Varambally S, et al. (2005) Integrative genomic and proteomic analysis of prostate cancer reveals signatures of metastatic progression. *Cancer Cell* 8:393–406.
6. Lapointe J, et al. (2004) Gene expression profiling identifies clinically relevant subtypes of prostate cancer. *Proc Natl Acad Sci USA* 101:811–816.
7. LaTulippe E, et al. (2002) Comprehensive gene expression analysis of prostate cancer reveals distinct transcriptional programs associated with metastatic disease. *Cancer Res* 62: 4499–4506.
8. Holzbeierlein J, et al. (2004) Gene expression analysis of human prostate carcinoma during hormonal therapy identifies androgen-responsive genes and mechanisms of therapy resistance. *Am J Pathol* 164:217–227.
9. Yu YP, et al. (2004) Gene expression alterations in prostate cancer predicting tumor aggression and preceding development of malignancy. *J Clin Oncol* 22:2790–2799.
10. Tomlins SA, et al. (2007) Integrative molecular concept modeling of prostate cancer progression. *Nat Genet* 39:41–51.
11. Taylor BS, et al. (2010) Integrative genomic profiling of human prostate cancer. *Cancer Cell* 18:11–22.
12. Sanchez-Carbayo M, Socci ND, Lozano J, Saint F, Cordon-Cardo C (2006) Defining molecular profiles of poor outcome in patients with invasive bladder cancer using oligonucleotide microarrays. *J Clin Oncol* 24:778–789.
13. Richardson AL, et al. (2006) X chromosomal abnormalities in basal-like human breast cancer. *Cancer Cell* 9:121–132.
14. Notterman DA, Alon U, Sierk AJ, Levine AJ (2001) Transcriptional gene expression profiles of colorectal adenoma, adenocarcinoma, and normal tissue examined by oligonucleotide arrays. *Cancer Res* 61:3124–3130.
15. Sabates-Bellver J, et al. (2007) Transcriptome profile of human colorectal adenomas. *Mol Cancer Res* 5(12):1263–1275.
16. Estilo CL, et al. (2009) Oral tongue cancer gene expression profiling: Identification of novel potential prognosticators by oligonucleotide microarray analysis. *BMC Cancer* 9:11.
17. Bhattacharjee A, et al. (2001) Classification of human lung carcinomas by mRNA expression profiling reveals distinct adenocarcinoma subclasses. *Proc Natl Acad Sci USA* 98: 13790–13795.
18. Talantov D, et al. (2005) Novel genes associated with malignant melanoma but not benign melanocytic lesions. *Clin Cancer Res* 11(20):7234–7242.
19. Segal NH, et al. (2003) Classification and subtype prediction of adult soft tissue sarcoma by functional genomics. *Am J Pathol* 163:691–700.
20. Segal NH, et al. (2003) Classification of clear-cell sarcoma as a subtype of melanoma by genomic profiling. *J Clin Oncol* 21:1775–1781.
21. Liao YL, et al. (2008) Identification of SOX4 target genes using phylogenetic footprinting-based prediction from expression microarrays suggests that overexpression of SOX4 potentiates metastasis in hepatocellular carcinoma. *Oncogene* 27:5578–5589.
22. Xu L, et al. (2008) Gene expression changes in an animal melanoma model correlate with aggressiveness of human melanoma metastases. *Mol Cancer Res* 6:760–769.
23. Radvanyi L, et al. (2005) The gene associated with trichorhinophalangeal syndrome in humans is overexpressed in breast cancer. *Proc Natl Acad Sci USA* 102:11005–11010.
24. Ki DH, et al. (2007) Whole genome analysis for liver metastasis gene signatures in colorectal cancer. *Int J Cancer* 121:2005–2012.

A

Characteristics of The Johns Hopkins University Progression Cohort Recurrence Cases and Matched Controls (n=136)			
	Cases N=68	Controls N=68	*P*
Mean ± standard deviation age (years)	59.2 ± 6.5	59.4 ± 5.9	Matched
White (%)	77.9	83.8	Matched
Median calendar year of surgery	1997.5	1994	< 0.0001*
Positive surgical margins (%)	35.3	23.5	0.13**
Pre-surgery PSA concentration (ng/mL)			
Mean ± standard deviation	12.0 ± 10.1	9.7 ± 6.7	0.20***
Median (Interquartile range)	9.8 (6.2-13.3)	7.9 (5.7-12.4)	0.12*
Pathologic Gleason sum (%)			
6	27.9	27.9	
7	44.1	44.1	Matched
8+	28.0	28.0	
Pathologic stage groups (%)			
T2	19.1	19.1	
T3a	44.1	44.1	Matched
T3b or worse	36.8	36.8	
Frist type of recurrence (%)			
Biochemical	57.4	--	
Clinical	42.6	--	

* From Wilcoxon sign rank test.
** Chi-squared Test.
*** Test of no difference in geometric means.

B

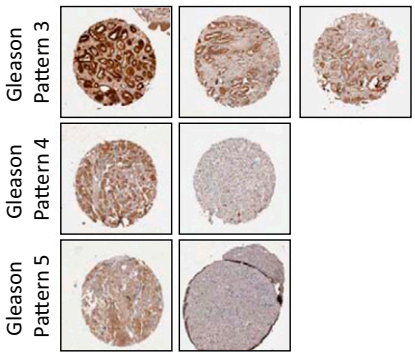

C

Johns Hopkins University Progression Cohort (n=136)

Model	Parameter	Hazard Ratio	P Value
More than 2 Cores Below the Median*	Number of Tumor Cores	3.48 (1.02, 11.85)	0.046
Number of Cores Below 25th Percentile	Number of Tumor Cores	1.59 (1.02, 2.47)	0.04
Number of Cores Below 25th Percentile*	Number of Tumor Cores	1.80 (1.09, 2.97)	0.02
Any Core Below 25th Percentile	Any Tumor Core	6.97 (1.38, 35.18)	0.02
Proportion of Cores Below 25th Percentile	Proportion of Tumor Cores	6.83 (1.18, 39.56	0.03
Number of Cores Below Median	Number of Tumor Cores	1.53 (1.06, 2.22)	0.03
Number of Cores Below Median*	Number of Tumor Cores	1.83 (1.15, 2.91)	0.01
Proportion of Cores Below Median	Proportion of Tumor Cores	6.75 (1.44, 31.58)	0.02

Restricted to subjects who had 3 or more cores (n=136; 68 case and 68 controls)
*Additionally controlled for number of cores tested

Fig. S7. Multivariable analysis of the JHU cohort demonstrates that loss of SPARCL1 expression is independently associated with prostate cancer recurrence. (*A*) Characteristics of the JHU progression cohort recurrence cases and matched controls. Recurrence cases as measured by biochemical recurrence (PSA ≥0.2 ng/mL), metastasis, or prostate cancer death after surgery were matched by Gleason sum, pathologic stage, age, and race/ethnicity to nonrecurrent controls. Conditional logistic regression was used to estimate the odds ratio of recurrence taking in account the matching factors and adjusting for year of surgery, presurgical PSA level, positive surgical margins, and residual difference in pathologic stage and grade (*n* = 136). (*B*) Variation of SPARCL1 expression within Gleason grade. SPARCL1 expression varies within Gleason grade as measured by IHC. (*C*) SPARCL1 protein expression was determined by IHC and quantified using TMAJ software on a series of TMAs containing prostate adenocarcinomas matched for Gleason grade, pathologic stage, age, and race/ethnicity, but differing in recurrence as measured by biochemical recurrence (PSA ≥0.2 ng/mL), metastasis, or prostate cancer death after surgery from the JHU progression cohort (*n* = 136). Multiple parameters of SPARCL1 expression criteria in multivariate analysis show the loss of SPARCL1 expression in prostate adenocarcinomas is significantly associated with prostate cancer recurrence independent of Gleason grade, pathologic stage, age, race/ethnicity, PSA, and other clinical variables.

A

Characteristics of Mayo Clinic High Risk Progression Cohort (n=235)

Events	%
BCR	53
METS	31
PCSM	14
GS > 7	41
SMS	57

B

Mayo Clinic High Risk Progression Cohort (n=235)

Biochemical Recurrence	Hazard Ratio	*P* Value
SPARCL1	1.4006 (1.1102, 1.7669)	0.0045
log(pPSA)	1.0997 (0.7727, 1.5649)	0.5977
GS	1.7459 (0.9099, 3.3500)	0.0938
SVI	2.0379 (0.9138, 4.5447)	0.0819
ECE	1.8842 (0.8406, 4.2235)	0.1240
SMS	1.2935 (0.6992, 2.3929)	0.4122

Metastatic Recurrence	Hazard Ratio	*P* Value
SPARCL1	1.6187 (1.2242, 2.1404)	0.0007
log(pPSA)	1.0608 (0.7083, 1.5887)	0.7746
GS	2.6351 (1.3490, 5.1472)	0.0046
SVI	2.1412 (1.0105, 4.5373)	0.0469
ECE	2.0710 (0.9747, 4.4004)	0.0583
SMS	1.1242 (0.5666, 2.2307)	0.7377

PCSM	Hazard Ratio	*P* Value
SPARCL1	1.7700 (1.2177, 2.5726)	0.0028
log(pPSA)	0.9049 (0.5122, 1.5987)	0.7307
GS	4.7750 (1.9125, 11.9217)	0.0008
SVI	1.6906 (0.6461, 4.4238)	0.2846
ECE	3.8669 (1.4325, 10.4380)	0.0076
SMS	1.2072 (0.5188, 2.8088)	0.6621

C

Mayo Clinic Gleason Sum 7 Progression Cohort (n=119)

Metastatic Recurrence	Hazard Ratio	*P* Value
SPARCL1	1.553601 (1.041589, 2.317301)	0.030795
log(pPSA)	1.297945 (0.7301, 2.30744)	0.374347
SVI	2.479037 (0.524261, 11.72245)	0.252081
ECE	2.416273 (0.730768, 7.989369)	0.148205
SMS	1.510108 (0.331098, 6.887475)	0.594481

Mayo Clinic Gleason Sum ≥8 Progression Cohort (n=98)

Metastatic Recurrence	Hazard Ratio	*P* Value
SPARCL1	1.861667 (1.046075, 03.31315)	0.03459
log(pPSA)	0.891099 (0.348264, 2.280044)	0.809914
SVI	2.586517 (0.842849, 7.93745)	0.09669
ECE	2.572674 (0.573738, 11.53602)	0.217102
SMS	1.189607 (0.380402, 3.720183)	0.765348

Fig. S8. Multivariable analyses of the Mayo Clinic cohort demonstrate that *SPARCL1* expression is significantly prognostic of BCR, MET, and PCSM. (*A*) Characteristics of the Mayo Clinic high-risk progression cohort. The percentage of BCR as defined by two consecutive increases of ≥0.2 ng/mL PSA after radical retro-pubic prostatectomy, MET as defined by a positive CT or bone scan, PCSM, Gleason sum (GS), and positive surgical margins (SMS) events in the dataset (n = 235). (*B*) Multivariable Cox regression survival analyses for *SPARCL1* gene expression in the Mayo Clinic high-risk prostate cancer progression cohort for BCR, MET, and PCSM endpoints (n = 235). Gleason sum, seminal vesicle invasion (SVI) (pathologic stage), extracapsular extension (ECE) (pathologic stage), and positive surgical margins (SMS). (*C*) Multivariable Cox regression survival analyses of the Mayo Clinic cohort stratified by Gleason sum (7, n = 119 and ≥8, n = 98) demonstrate that *SPARCL1* gene expression is significantly prognostic of MET.

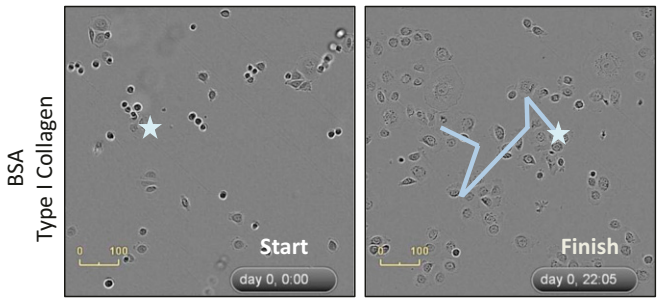

Movie S1. SPARCL1 inhibits type I collagen induced adhesion and migration. PC3 cells were seeded on a type I collagen/BSA matrix. Time-lapse microscopy monitored cellular adhesion and migration for 22 h.

Movie S1

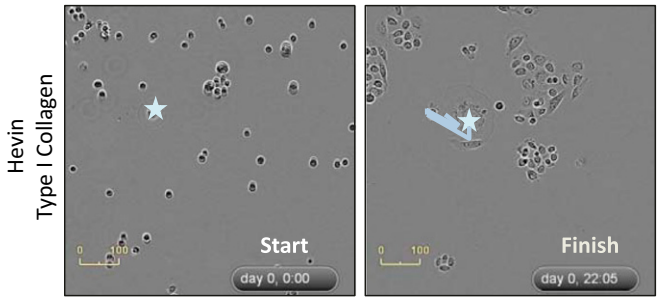

Movie S2. SPARCL1 inhibits type I collagen induced adhesion and migration. PC3 cells were seeded on a type I collagen/SPARCL1 matrix. Time-lapse microscopy monitored cellular adhesion and migration for 22 h.

Movie S2